Modeling thermal effects on bridge dynamic responses.

Etienne Balmes[1,2], Mathieu Corus[1], Dominique Siegert[3]
[1]*Ecole Centrale Paris/MSSMat*, [2]SDTools, [3]LCPC
balmes@sdtools.com

ABSTRACT

The paper seeks to analyze the influence of temperature on the dynamic behavior of bridges. The objective is to propose a model that can be used to analyze the validity of damage detection algorithms that seek to separate variations in the modal properties due to damage or temperature. One first shows how temperature changes generate thermal stresses which, depending on the boundary conditions, can generate pre-stress levels that are sufficient to induce frequency shifts in the response. A procedure to compute these effects and generate low dimension reduced models with temperature appearing explicitly is proposed. This procedure is then illustrated for a simplified bridge and a realistic one for which test results are available.

1 INTRODUCTION

Temperature changes are known to affect the dynamic properties of bridges significantly so that the issue of rejecting the effects of such changes in damage detection techniques has raised significant interest. Most of the work in this area has been experimental, so that it appeared useful for the community of people developing in-operation data analysis methods to provide a sample model that would present both temperature effects and damage cases. Describing this model is the objective of this paper.

Section 2 present the theoretical framework used to model the effect of thermal loads and generate reduced parametric models that account for the dynamics of a system under thermal loads and damage represented as a multiplicative coefficient on the stiffness matrix of a subset of elements.

This model is generated using functions of the OpenFEM [1] and the Structural Dynamics Toolbox [2]. The format of the reduced model is described so that people can validate their methods without these software packages. The script associated with the article is available at

www.sdtools.com/support/sdtdemos/bridge_with_thermal.m

Section 3.1 gives a first application on a simplified bridge showing the influence of boundary conditions and variations in bridge section on the thermal sensitivity. Section 3.2 analyzes the more realistic case of a pre-stressed concrete guider bridge on motorway north near Paris tested in ambient excitation conditions due to the traffic.

2 THEORY

2.1 Thermal and pre-stress effects

The presence of a thermal field generates an expansion of materials associated with a thermal strain $[\epsilon_T] = \alpha(T - T_0)[I]$, which can be related to a thermal stress field using the elastic constitutive law

$$\sigma_T = C : \epsilon_T = \lambda Tr(\epsilon_T)I + 2\mu\epsilon_T \tag{1}$$

The thermoelastic equilibrium as solution of the problem

$$\{\delta v\}^T[K]\{q_T\} = \int_\Omega \sigma_e(q_T) : \epsilon(\delta v) = \int_\Omega \sigma_T : \epsilon(\delta v) \quad \forall \quad \delta v = \{\delta v\}^T\{F_T\} \tag{2}$$

The effect of a temperature modification thus appears as an external load F_T corresponding to the right hand side of (2). Solving equation (2), with appropriate boundary conditions, leads to $\{q_T\}$ the static equilibrium of the structure under thermal loading.

This equilibrium may or not be associated with pre-stress. This is easily understood with the case of a uniform temperature elevation in a bar. If the bar is free, it simply expands and there is no induced stress (the shape changes a little but if deformations are small the stiffness matrix is unaffected and the frequencies don't change). If the bar extremities are fixed, it cannot expand and the temperature elevation induces pre-stress. This affects the stiffness and thus the modal frequencies.

For a given prestress state given by the difference between the elastic stress associated with the static equilibrium under thermal loading $\sigma_e(q_T)$ and the thermal stress $\sigma_T(\epsilon_T)$, one can compute the geometric stiffness matrix

$$K_\sigma(q_T, \epsilon_T) = \int_\Omega (\sigma_{ij,e}(q_T) - \sigma_T)\, u_{k,i} v_{k,j} \tag{3}$$

and the modes of the heated structure are now given by

$$\big[K + K_{\sigma(q_T,\epsilon_T)} - \omega_j^2 M\big]\{\phi_j\} = \{0\} \tag{4}$$

In the case of bridge pre-stressed by cables, one should also include these contributions when computing K_σ. This has not been done here but one can expect the differential influence of temperature on pre-stress cables and concrete to have some influence since the thermal expansion coefficients are slightly different ($1.26e-5$ for steel, vs. $1.2e-5$ for concrete).

2.2 Reduced models of the effects of temperature

Assuming that thermal loads induce small mechanical perturbations, it clearly appears in equations (2)-(3) that q_T, $\sigma(q_T)$ and K_{σ_T} are a linear functions of the thermal field $T(x)$. If the thermal field itself is described as a linear combination of constant thermal fields $\{T(x)\} = \sum_i \{T_i(x)\} p_i$, the effect of temperature on the stiffness matrix can be written as

$$[K(p_i)] = [K(T_0)] + \sum_i p_i [K_{\sigma_{Ti}}] \tag{5}$$

The effect of temperature on modeshapes, thus takes the form of a classical parametric eigenvalue problem described by a linear combination of constant matrices. Methods to approximate such problems are discussed in Refs. [3, 4, 5].

To generate a small size parametric model, one retains a multi-model strategy [4] by computing target modes at the reference temperature and with a unit thermal load. The model is then reduced on the basis

$$[T] = [\phi_{1:NM}(T_0) \quad \phi_{1:NM}(T_0 + 1 \times T_i)]_{orth} \tag{6}$$

where the *orth* refers to the fact that a full orthonormalization procedure is performed to generate independent mass orthonormal and stiffness orthogonal vectors [5].

2.3 Damage models

The authors are not aware of any comprehensive study on realistic damages that would be of interest for detection in bridges. Cases cited in the literature are depression of piles, rupture of pretension cables, degradation of joints. In the absence of better approaches, simple multiplicative models on the stiffness of parts of the bridge were retained. Such models are introduced as a proportionality coefficient for a group of elements. Thus the final model considers thermal and stiffness changes with

$$[K(p_i)] = [K(T_0)] + \sum_i p_i [K_{\sigma_{Ti}}] + p_k [K_{Damage}] \tag{7}$$

The reduction basis is augmented to account for the damage effect using a first order correction strategy, where the additional vectors appended to (6) are given by

$$[T] = [K(0)]^{-1} [\Delta K] \phi_{1:NM}(T_0) \tag{8}$$

2.4 Format of the reduced parameterized models

Computations are performed in the SDT environment [2] using recent developments of OpenFEM [1] to account for geometric non-linearities and prestress effects in the 3D volume element families. The resulting reduced models can be found at ftp.sdtools.com/contrib/bridge_thermal_*.mat

Each is described by a data structure `MVR` with the following fields

```
          K: {1x5 cell}     % reduced matrices
       Klab: {1x5 cell}     % names for reduced matrices
         TR: [1x1 struct]   % reduction basis T
  zCoefFcn: 'zCoef=[-w.^2 ones(length(w),1)*(1+2e-2*i)*[1 par]];'
         cr: [15x80 double] % observation matrix for outputs
    lab_out: {15x1 cell}    % output names
         br: [80x1 double]  % input matrix for applied force
     lab_in: {'in'}
```

The reduced model is thus characterized by an identity mass $T^T M^T = I$ (`MVR.K{1}`), a diagonal nominal stiffness $T^T K(T_0) T$ (`MVR.K{2}`), non diagonal thermal coupling matrices $T^T K_{\sigma_{T_i}} T$ and damage representations. Inputs and outputs at arbitrary positions can easily be generated using the projection of input/output shape functions

$$\{y\}_{NS} = [c]_{NS\times N}\{q\}_N = [c]_{NS\times N}[T]_{N\times NR}\{q_r\}_{NR} \tag{9}$$

To compute the response in a given operating condition, one uses

```
coef=[-20 ... % uniform shift from 20 C
      5   ... % gradient deck at 20+5, bottom at 20-5 C
      .7];    % multiplicative coefficient on damage model
KR=MVR.K{2}+coef(1)*MVR.K{3}+coef(2)*MVR.K{4}+coef(3)*MVR.K{5};
[mdr,fr]=fe_eig(MVR.K{1},KR);
def=MVR.TR; def.def=def.def*mdr;  % modeshapes at all DOFs
```

3 APPLICATIONS

3.1 Simplified bridge

As a first application, one considers a simplified bridge model with a deck that is 3 meter high,6.6 to 10 m wide shown in figure 1. The 60 m span is modeled using 9600 volume elements and 13668 nodes. Material properties used are $E = 40GPa, \nu = .17, \rho = 2200kg/m^3, \alpha_T = 1.210^{-5}(^oC)^{-1}, T_0 = 20^oC$. At the extremities of the span, motion is blocked in the y and z directions while a nominal stiffness of $1e10N/m$ is used, in the bridge x direction, to simulate a blocking condition.

The temperature variations are modeled using two fields: a uniform temperature elevation and a linear variation with z from 25^oC on the deck to 15^oC at the bottom. The ability to represent actual temperature states using a linear combination of these two fields is an open question that will be addressed in another study.

Figure 1 illustrates the vertical thermal gradient field and the induced axial strain σ_{xx} state. The warmer deck tends to expand while the cooler bottom contracts. The figure also clearly shows edge effects where the springs used to model attachment conditions near the piles.

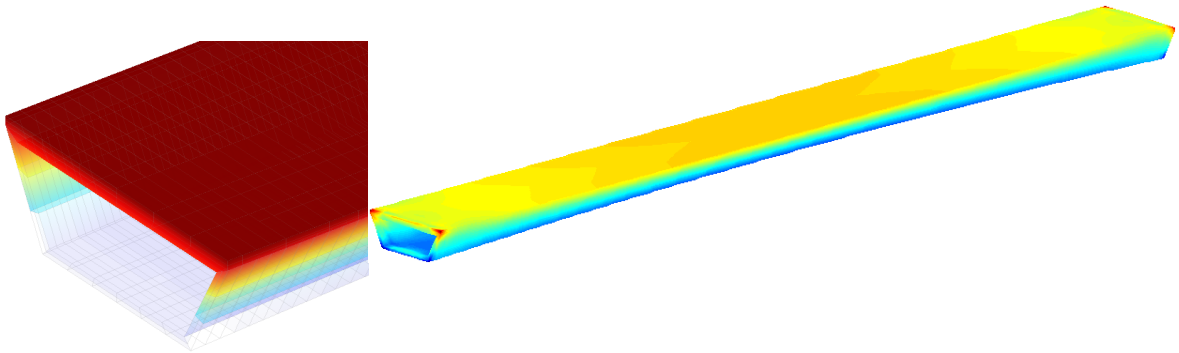

Figure 1: Linear thermal field on the bridge model and induced axial stress

Figure 2 illustrates effects of temperature changes on a particular transfer function. The uniform temperature increase has a more significant effect where frequencies decrease with temperature. This is expected trend is the span is attached with stiff springs at the extremities. Thus heating generates a compressive axial load that decreases frequencies. The effect of gradients is smaller but shifts frequencies in the opposite direction.

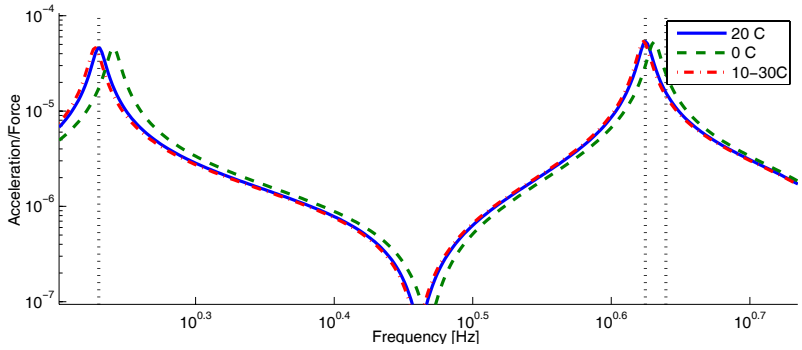

Figure 2: Effects of temperature on a transfer function from the edge of the bridge.

Table 1 analyses the effect of boundary conditions of the bridge span. It appears that the sensitivity to uniform temperature elevations is smaller when the span extremities are attached to springs. This is a rather surprising result since the frequencies of a free-free beam are expected not change with temperature. Figure 3 illustrates the horizontal motion of the bridge under a uniform temperature elevation. If the bridge had a uniform section, one would expect no motion at all for fixed extremities. Here the variable section induces bending of the bridge under this uniform temperature elevation. The x axis motion is a result of this elevation. The plot also shows that there are strong variations of the axial stress through the bridge, which probably account for the effects on temperature sensitivities.

TABLE 1: Frequency shifts (in %) for transition from 20C to 0C and 30-10C gradient. Cases with axial springs and without

	Uniform+Kx	Gradient+Kx	Uniform	Gradient
1st z-ending	2.4532	-0.6163	5.0267	-1.2483
2nd z-bending	1.4432	-0.3371	0.8205	-0.1817
y-bending	0.3465	-0.0747	2.3511	-0.5400
Torsion	0.9110	-0.2164	1.2688	-0.2923
y-bending	0.0413	-0.0274	0.3108	-0.0689
3rd z-bending	0.1882	-0.0404	0.0438	-0.0261

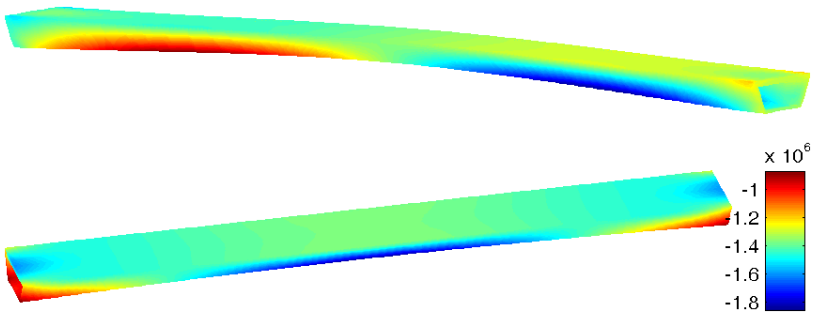

Figure 3: Top: X motion under uniform temperature elevation. Bottom: variations of axial stress due to thermal load.

3.2 Prestressed concrete bridge

This second model corresponds to the case of a pre-stressed concrete guider bridge with independent spans, on motorway near Paris, which was tested under ambient excitation during a six month period. Each VIPP span is 33 by 12.4 meter with five braced I shaped pre-stressed beams and a top deck as shown in figure 4 (which shows two parallel bridges). The instrumented span is connected to an expansion joint at the bank side and the top slabs at the other end are connected to ensure the continuity of the pavement.

The beams are supported by laminated rubber bearings with an horizontal/shear stiffness $1e7N/m$ and vertical stiffness of $2.4e9N/m$ [6]. The dependence of these nominal stiffness values on temperature is not well known. This system allows the transmission of horizontal forces while leaving beam rotations relatively free.

Figure 4: Picture of the tested bridge. Only one of the two bridges was modeled/tested.

The FEM model shown in figure 5 contains 8 400 nodes and 4300 volume elements. The rubber connections to the piles and the attachment to the neighboring spans are modeled using elastic springs (shown as circles).

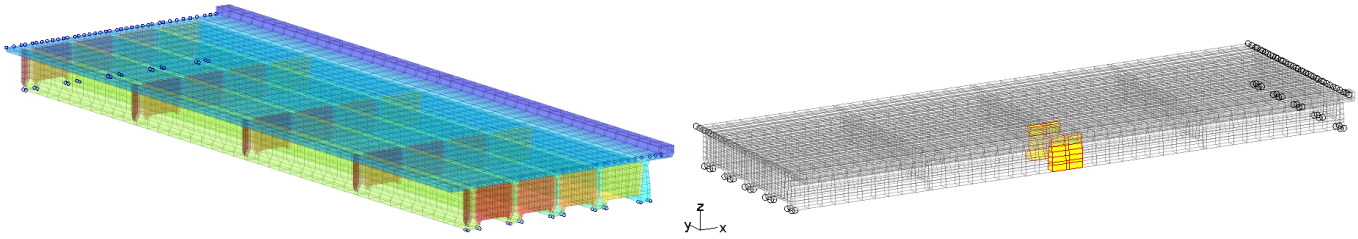

Figure 5: FEM model of the Roberval bridge. Localization of the considered damage case.

The damage is modeled as a reduction of the concrete modulus by up to 30 % on the external beams P1 and P2 over a length of 1 m. These beams are more heavily loaded because of truck traffic on the slow lane, which motivated the chosen damage localization.

During the six month test a number of in operation measurements were performed which allowed the extraction of modal properties using the COSMAD toolbox[7] for Scilab. Figure 6 shows that there is a clear correlation between external temperature and frequency of the first two modes (bending and torsion that were well excited by truck traffic).

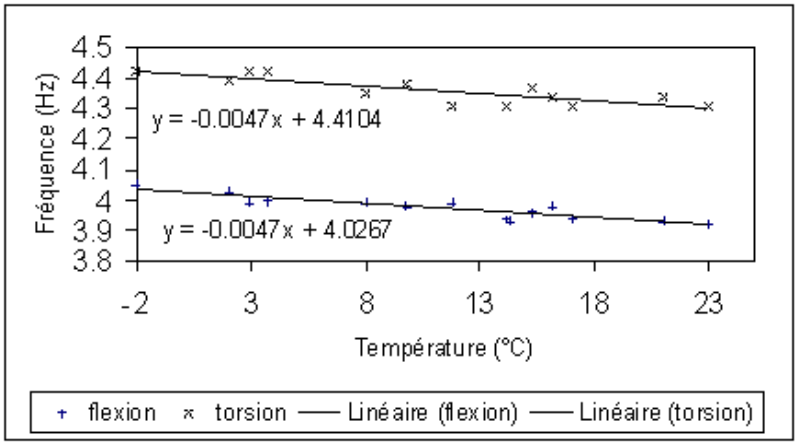

Figure 6: Experimental correlation between frequencies and temperature.

The thermal state is again modeled using a combination of a uniform temperature increase and a linear variation with z. Figure 7 shows of the transformation of the parametric hypercube (damage stiffness coefficient between .7 and 1, uniform temperature between 0 and 20 C, temperature gradient between 0 and 10 C. Similar information is reported in table 2.

The decrease of frequencies with temperature is properly predicted but the decrease in test is an order of magnitude larger. The bridge bearing being made of laminated rubber, one can expect majors effects of temperature [8]. The table shows the effect of a 30 % decrease in the bearing stiffness, which induces shifts that are closer to the test levels. This thus appears to be a realistic explanation for the relatively high influence of temperature. Other effects could come from span connections (sensitivity studies showed some influence), unmodeled pre-stress cables, ...

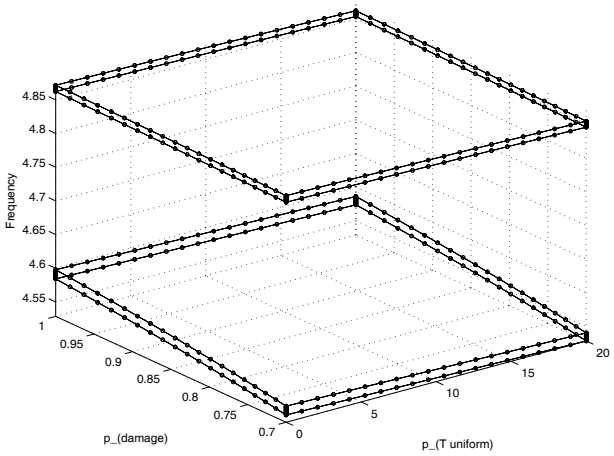

Figure 7: Predicted temperature/damage pole map.

TABLE 2: Frequency shifts (in %) for transition from 20C to 0C, 30-10C gradient, 30 % decrease in modulus for the damage area and the bearings.

	Uniform	Gradient	Damage	Bearing
z-bending	0.2563 (2.33 test)	-0.2693	-0.9898	-1.0267
Torsion	0.2064 (2.13 test)	-0.1758	-0.1400	-1.0228
y-bending	-0.0368	-0.0622	-0.1817	-4.0753
z-bending	0.1236	0.0041	-0.1240	-5.2782
torsion	0.1205	-0.0019	-0.0603	-4.3323
z-bending	-0.0152	-0.0328	-0.0076	-0.5726

A question that is often debated is whether modeshapes change. This can be easily studied by predicting the modified response using a reduction basis that only contains the modes of the nominal model. Table 3 clearly indicates that frequency shifts due to temperature are still well predicted while the effects of the damage is significantly under-predicted. It thus appears that the considered damage case modifies modeshapes while the thermal effects have little influence.

TABLE 3: Frequency shifts (in %) for transition from 20C to 0C, 30-10C gradient, 30 % decrease in modulus for the damage area and the bearings. *Approximation on the basis of nominal modes*.

	Uniform	Gradient	Damage
z-bending	0.2672	-0.2445	-0.7434
Torsion	0.2378	-0.1448	-0.1093
y-bending	-0.0364	-0.0617	-0.1368
z-bending	0.1261	0.0093	-0.0924
torsion	0.1251	0.0043	-0.0497
z-bending	-0.0149	-0.0324	-0.0056

4 CONCLUSION

This work showed that modeling of temperature effects in bridges could be achieved. Correlation with tests indicated that frequency shifts due to temperature tended to be of the same order than shifts due to large damages. This confirms the need for study of this topic.

5 ACKNOWLEDGEMENTS

This work was done with partial funding from ACI Constructif.

REFERENCES

[1] **INRIA** and **SDTools**, OpenFEM, a finite element toolbox for Matlab and Scilab, INRIA, Rocquencourt, France, www-rocq.inria.fr/modulef, SDTools, Paris, France, www.sdtools.com, 2004.

[2] **Balmes, E.** and **Leclère, J.**, Structural Dynamics Toolbox 5.1 (for use with MATLAB), SDTools, Paris, France, www.sdtools.com, October 2003.

[3] **Balmes, E.**, *Parametric families of reduced finite element models. Theory and applications*, Mechanical Systems and Signal Processing, Vol. 10, No. 4, pp. 381–394, 1996.

[4] **Balmes, E.**, *Uncertainty propagation in experimental modal analysis*, IMAC, Dearborn, 2004.

[5] **Bobillot, A.**, Méthodes de réduction pour le recalage. Application au cas d'Ariane 5, Ph.D. thesis, École Centrale Paris, 2002.

[6] **SETRA**, Appareils d'appui à pot de caoutchouc. Utilisation sur les ponts, viaducs et structures similaires - Guide technique, Guide Technique SETRA, 2000.

[7] **Mevel, L., Goursat, M.** and **Basseville, M.**, *Detection for in-operation structures: a Scilab toolbox use of the GUI for the localization*, International Modal Analysis Conference XXII - Dearborn, MI.

[8] **Nashif, A., Jones, D.** and **Henderson, J.**, Vibration Damping, John Wiley and Sons, 1985.